Int. J. Electrochem. Sci., 14 **(2019)** 2714 – 2731, doi: 10.20964/2019.03.16

International Journal of
ELECTROCHEMICAL
SCIENCE
www.electrochemsci.org

Influence of Soybean (Glycine Max) Plant Extract on Corrosion of Aluminum in 1M HCl

Ali M. El-Azaly

Nile Higher Institute for Engineering and Technology, El-Mansoura, Egypt
E-mail: dr_alielazaly_81@yahoo.com

Received: 17 October 2018/ *Accepted:* 15 December 2018 / *Published:* 7 February 2019

Glycine Max Extract (G.M.E.) is used as a corrosion inhibitor for aluminum alloy in 1.0M HCl employing chemical (weight loss, WL) and electrochemical (Potentiodynamic polarization, PP, electrochemical frequency modulation, EFM and AC impedance, EIS techniques. The scanning electron microscope (SEM) was used to examine the surface morphology of Al alloy. The temperature effect on corrosion the rate in the presence of various concentrations was measured in the range of 298-318K by WL. PP curves demonstrate that G.M.E is a mixed type inhibitor. The corrosion efficiency improved by raising GM.E concentration and with improving temperature. Temkin's isotherm was established to be the best isotherm to define the adsorption of the G.M.E. on the surface of Al alloy. The adsorption and activation parameters had calculated and discussed.

Keywords: HCl, Aluminum alloy, Glycine Max Extract (G.M.E.), SEM. EFM, EIS

1. INTRODUCTION

The corrosion process is considered a fundamental process, which plays a vital character in safety and economics, especially for metals. The best one test for corrosion inhibition the use of inhibitors, exclusively in acidic media [1]. On the other hand, acids enhance the rate of metal dissolution and are responsible for material failure indirectly. So, adding a corrosion inhibitor is an important method in order to decrease metal dissolution in such solutions. Most of the well-known acid inhibitors are organic compounds containing nitrogen, sulfur, and oxygen [2-5]. For the corrosion inhibition of aluminum [6-8], organic heterocyclic compounds have been used as well as for copper [9], iron [10-13] and other metals [14-15] in various corrosive media. Though a lot of these organic heterocyclic assembled have great protection efficiencies, many of them have unwanted side effects, until if they are in minor concentrations, because of their toxicity to the environment or humans, besides being expensive [16]. An economic and safe environment is the chief advantages for utilizing extracts as corrosion protection. Thus far, numerous wild extracts have utilized as corrosion hindrance

for Al alloy in acidic solution, for instance [17] were studied as a corrosion inhibitor for aluminum in HCl solution. Ebenso et al. [18] showed that the ethanolic extract of Carica papaya and Azadirachtaindica are good corrosion inhibitors for Al in HCl solution. The inhibitive effect of tobacco plant on Al corrosion in HCl was investigated before [19]. The stem of the Opuntia [20] extract was reported as inhibitor for the corrosion of Al in HCl solution. Punica Granatum plant extract [21], Salicornia Begolovi [22] were used as corrosion inhibitors for Al in 1 M HCl. Glycine Max (L.) common name is soybean which is considered to be a major leguminous crop, cultivated globally as well as in Iran. Soybean essential oil has an antioxidant and antimicrobial activities of seeds on various plant pathogens that cause damages to crops [3]. Also used for cardiovascular disease, cancer and renal function [23].

2. MATERIAL AND METHODS

2.1. Materials and solutions

The chemical composition of the used Al alloy (% weight) is: Fe 0.60, Si 0.30, Mg 0.05, 1.40 Mn, 0.100 Cu, 0.05 Ti, 0.05 Cr and the rest is Al alloy. The Pt wire (1 cm^2) and saturated calomel electrode (SCE) was utilized in an electrochemical cell as counter and reference electrodes, respectively. Dilution of the reagent grade 34% HCl with bi-distilled water was made for preparation of the aggressive solution. A Glycine Max (1000 ppm) stock solution was used in order to prepare the required concentrations. Glycine Max concentrations used were 50,100,150,200,250.300 ppm.

2.2. Glycine Max Extract (G.M.E.) Preparation

The dried sumac seeds sample were ground into a fine powder in a blender. (100 g) of powder sumac mixed with 500 ml boiling bidistilled water with stirring for 15 min, then the aqueous extract was filtrated. The filtrates were frozen at -84^{0}C. More analysis has illustrated that the main chemical constituents of Glycine Max are Genistein, Daidzein and Biochanin A [24] as shown in scheme1.

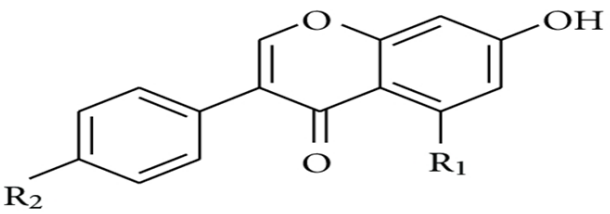

	R_1	R_2
Genistein	OH	OH
Daidzein	H	OH
Biochanin A	OH	OCH_3

Scheme 1. Chemical structure of compounds from Glycine max

2.3. Weight Loss (WL) Measurements

Seven equivalent Al alloy coins of 2 x 2 x 0.2 cm were polished with emery papers (grade 340-600-12000 then washed using acetone and water bi-distilled. The immersion of the specimens was taking place in a beaker 250 ml, which enclosed 100 ml HCl in presence and absence of Glycine Max in different concentrations, after accurate weighing. The protection efficiency (IE %) and θ of G.M.E were measured as shown in equation 1: [23]

$$IE\% = \theta \text{ x } 100 = \left[1 - \frac{W}{W^o}\right] x\ 100 \qquad (1)$$

Where, the values of the average WL's are expressed by W and W^o with and without adding the inhibitor, in that order.

2.4. Electrochemical techniques

2.4.1. Potentiodynamic Polarization Measurements

Electrochemical tests were accomplished utilizing a special three-compartment glass cell consisting of the Al alloy coins as the working electrode (WE) (1 cm^2). Under unstirred conditions, all the tests were performed in open system solutions. Before each experiment, all potential data were recorded versus SCE, emery paper with successive different grades was used in order to abrade the electrode, then the electrode was degreased utilizing acetone, washed using water bi-distilled and finally, dried. The potential sweeping from -800 mV to -500 mV, at 1 mVs^{-1} scan rate with respect to E_{oc} , open circuit potential. For the calculate of corrosion current, Stern-Geary test [26] was carried out by anodic and cathodic extrapolation to data which give (log i_{corr}) and give (E_{corr}) which express the equivalent corrosion potential for hindrance free acid and for each G.M.E. concentration. i_{corr} was utilized for determination of surface coverage (θ) and inhibition efficiency (IE%) as in the next equation 2:

$$IE\% = \theta \text{ x } 100 = \left[1 - \frac{i_{corr(inh)}}{i_{corr(free)}}\right] x\ 100 \qquad (2)$$

Where, the corrosion current densities are expressed by $i_{(corr(free))}$ and $i_{(corr(inh))}$ without and with of inhibitor, in that order.

2.4.2. Electrochemical Impedance Spectroscopy (EIS) Measurements

By using AC signals, impedance measurements were accomplished in a range of ($2x10^4$ Hz to $8x10^{-2}$ Hz) frequencies with 10 mV peak to peak amplitude at OCP. Based on the equivalent circuit, the impedance was examined and explained. R_{ct} is the charge transfer resistance and C_{dl} is the capacitance double layer. These are the main parameters obtained from Nyquist diagram analysis. These parameters data obtained from the calculated of impedance measured from equation 3 as follows:

$$IE\% = \theta \text{ x } 100 = \left[1 - \frac{R_{ct}^o}{R_{ct}}\right] x\ 100 \qquad (3)$$

Where the charge transfer resistances are expressed by R_{ct}^{o} and R_{ct} without and with inhibitor, in that order

2.4.3. Electrochemical Frequency Modulation (EFM) Measurements

EFM was accomplished using two frequencies (2 and 5 Hz). The waveform repeats after 1 s because 0.1 Hz represents the base frequency. The lower frequency must be no more than half the higher one. Harmonic and intermodulation current peaks illustrated current responses in the intermodulation spectra. (i_{corr}) which represents the corrosion current density, (β_a and β_c) which represent the Tafel slopes and the causality factors (CF-2 & CF-3) were computed using the large peaks [27]. In 30 min before the beginning of the measurements, stabilization of the electrode potential was allowed. At 25^{o}C, all the experiments were conducted. By using the instrument of Gamry (PCI4/750) Potentiostat/Galvanostat/ZRA, all electrochemical measurements were carried out. Gamry requests contain DC105, EIS 300 software, and EFM 140 software for PP, EIS and EFM tests by collecting data via computer, respectively. For drawing, graphing and fitting data, Echem 6.03 software was used.

2.5. Analysis of Al Alloy Surface

About morphological study, features of Al alloy surface were examined using the SEM JEOL JSM-5500 beforehand and afterward immersion in 1.0 M HCl for 24-hour with and without G.M.E.

3. RESULTS AND DISCUSSION

3.1. Weight Loss (WL) Technique

In the presence and absence of altered concentrations of G.M.E., WL tests were done for Al alloy in 1.0 M HCl and are shown in figure (2). The measured data of %IE are listed in the table (1). From this table, it is noted that IE% is directly proportional to the concentration of G.M.E and inversely proportional to the temperature rising from 25-45^{o}C. The detected G.M.E inhibition action could be referred to its components adsorption on the surface of Al alloy. The adsorbed molecules form a layer which isolates the aggressive medium away from the surface of Al by blocking the corrosion centers on the surface which limits the medium dissolution and then the corrosion rate decreases, by improving efficiency as their concentrations rise (table 2) [28].

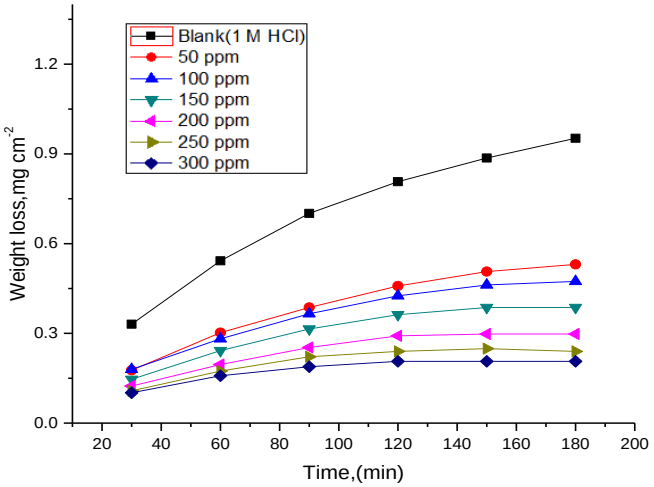

Figure 2. WL vs. time curves for Al alloy corrosion in HCl 1.0 M in the presence and absence of G.M.E. at 25°C

Table 1. (k_{corr}) corrosion rate, (Θ) and (IE %) variation with different concentrations of G.M.E at different temperatures after 120 minutes immersion

Temp. °C.	[Inh]. ppm	Θ	%IE
25	Blank	----	----
	50	0.498	49.77
	100	0.534	53.36
	150	0.603	60.29
	200	0.680	68.03
	250	0.737	73.73
	300	0.774	77.39
30	Blank	----	----
	50	0.398	39.78
	100	0.465	46.53
	150	0.553	55.27
	200	0.628	62.77
	250	0.689	68.88
	300	0.727	72.69
35	Blank	----	----
	50	0.363	36.30
	100	0.458	45.83
	150	0.555	55.45
	200	0.617	61.70
	250	0.675	67.47
	300	0.709	70.89
40	Blank	----	----
	50	0.327	32.74

	100	0.451	45.14
	150	0.556	55.63
	200	0.606	60.64
	250	0.660	66.05
	300	0.691	69.06
45	Blank	----	----
	50	0.291	29.11
	100	0.445	44.47
	150	0.558	55.80
	200	0.596	59.58
	250	0.646	64.61
	300	0.672	67.16

Table 2. Variation of the corrosion rate (C.R) and (%IE) with various concentrations of G.M.E from WL tests at 120 min dipping in HCl at 25ºC

[inh.] ppm	**(Glycine Max)**	
	%IE	**C.R $mg.cm^{-2}.min^{-1}$**
0	----	0.0076
50	50.0	0.0038
100	53.9	0.0035
150	60.5	0.0030
200	68.4	0.0024
250	73.7	0.0020
300	77.6	0.0017

3.2. Potentiodynamic Polarization (PP) Tests

Figure 3 shows the curves of PP for Al alloy in 1.0 M HCl solutions with and without various concentrations of G.M.E at 25ºC. Lee and Nobe [29] reported that during potential sweep experiments, a current peak occurred between Limiting-current regions and the apparent-Tafel. A remarkable decreasing in the rate of corrosion occurs due to the presence of G.M.E in 1.0 M HCl which shifts both the anodic and cathodic branches to the lesser data of the current densities of corrosion. From the PP diagrams in figure 3, the kinetic parameters are obtained in (table 3). The Tafel slopes β_a and β_c at 298 K do not change in presence of G.M.E. Generally, in case of presence of inhibitor, if the shift of corrosion potential is less than 85 mV, then the classification of the inhibitor can be a mixed kind [30, 31]. In our study E_{corr} changes about (20-30 mV) which are very small, this illustrates that G.M.E can acts as a mixed kind inhibitor.

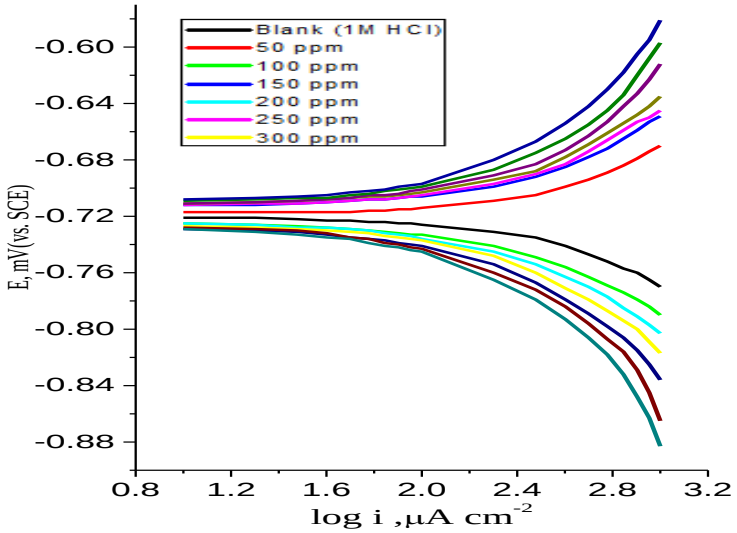

Figure 3. PP plots for the Al alloy corrosion in the absence and presence of various concentrations of G.M.E. at 25°C

Table 3. PP parameters for corrosion of Al alloy in 1.0 M HCl at 25°C

Inhibitor	[Inh] Ppm	$-E_{corr}$ mV vs. SCE	i_{corr} m A Cm^{-2}	β_a mV dec^{-1}	β_c mV dec^{-1}	C.Rx10^3 mpy	Ɵ	IE%
Blank	0	725	275	250	420	164	---	---
Glycine Max extract	50	724	138	80.0	68.0	289	0.498	49.8
	100	724	116	86.0	77.0	180	0.615	57.8
	150	725	102	90.0	87.0	84.7	0.631	62.9
	200	726	78.7	97.0	97.0	44.9	0.714	71.4
	250	726	58.3	105	100	37.9	0.788	78.8
	300	727	51.4	122	110	34.7	0.813	81.3

3.3. Electrochemical Impedance Spectroscopy (EIS) Measurements

Impedance curves for Al alloy in 1M HCl with and without various concentrations of G.M.E are shown in figure 4. A Nyquist semicircle type was found in the impedance spectra without the note of diffusive influence to the total impedance (Z), indicating that the presence of inhibitor does not change the corrosion reaction mechanism and undergoes mainly under charge-transfer. Due to the frequency dispersion, it was found that there was not a perfect semicircle obtained from Nyquist plots and this behavior due to the electrode surface roughness [32, 33]. Constant phase element (CPE) is considered the most widely employed. In universal, a CPE is utilized in a model in order to replace a capacitor to make up for the system [34]. It was established that the semicircle diameters are directly proportional to the concentration of G.M.E. This explains that the oxide layer increases the polarization resistance with increasing G.M.E concentration and the lower capacitive semicircle is regularly attributed to surface inhomogeneity and roughness [35]. The value illustrated that each EIS diagram contains a great capacitive loop with frequency dispersion in low values (inductive arc).

Generally, this inductive arc referred to anodic adsorbed intermediates controlling the anodic procedure [36-37].

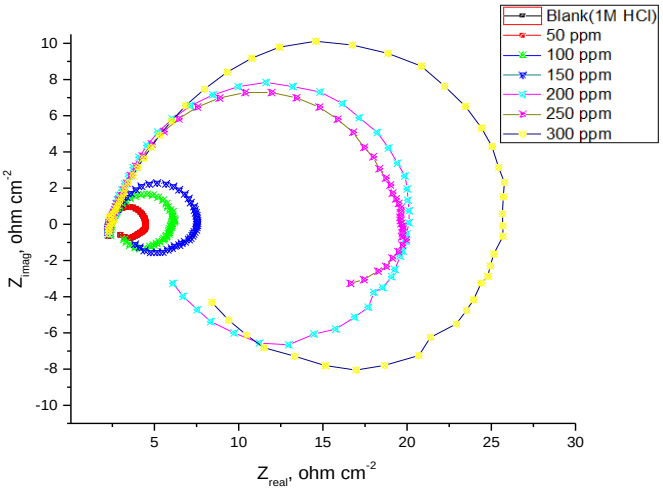

Figure 4. Nyquist curves of Al alloy in 1 M HCl solutions with and without altered concentration of G.M.E. at 25°C

Figure 5 shows the electrical circuit equivalent model which was utilized for analyzing the obtained impedance data. This model includes the (R_{ct}), (R_s) and (CPE). (n) is the frequency power data of CPE, can be supposed to parallel to capacitive performance. The permission of CPE is designated in equation 4 as follows:

$$Y_{CPE} = Y_o(j\omega)^n (4)$$

Where Y_o is the magnitude, J is the imagined root, ω is the angular frequency and n is the exponential term [36].

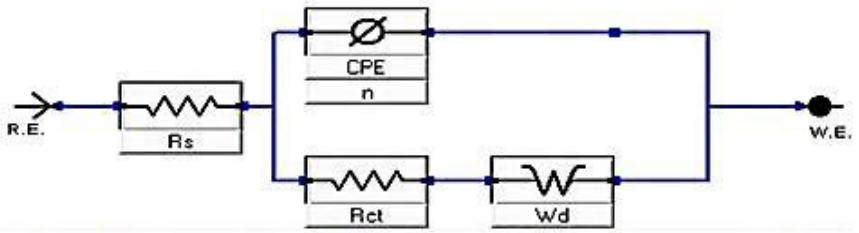

Figure 5. Equivalent circuit utilized to fit data of EIS for Aluminum alloy

Figure 4 shows the obtained data of the corrosion performance of Al in the presence and absence of G.M.E. In addition, Bode diagrams for the Al alloy were shown in figure 6. In which R_Ω is a great frequency limit corresponding to the electrolyte resistance while the lower frequency was the summation of ($R_\Omega + R_{ct}$), where R_{ct} is in the first estimate measure by both electrolytic conductances of the oxide film [39].

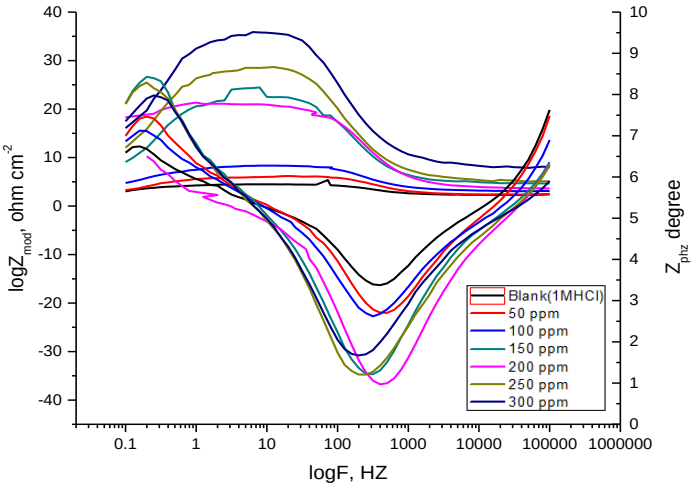

Figure 6. Bode curves for Al alloy in 1M HCl solutions in the presence and absence of different G.M.E. concentrations at 25°C

From the Nyquist diagram analysis, we deduced the following main parameters:

- R_{ct} which represents The charge transfer resistance (high frequency loop diameter)
- C_{dl} which represents The double layer capacitance and defined as:

$$C_{dl} = \frac{1}{2\pi R_{ct} f_{max}} \quad (5)$$

Where f_{max} is the maximum frequency at which the Z_{imag} of a maximum EIS.

Since $\frac{1}{R_{ct}}$ is directly proportional to C_{dl} (double layer capacity) according to the electrochemical theory, the (IE %) of protection of Al alloy in 1.0 M HClwas measured from R_{ct} data which are given by the impedance value at various concentrations of the used inhibitor as the next:

$$\%IE = \left(1 - \frac{R_{ct}^{o}}{R_{ct}}\right) x\ 100 \quad (6)$$

Where charge transfer resistance is expressed by R_{ct}^{o} and R_{ct} in the without and with of G.M.E, in that order.

From (table 4) which gives the impedance data, we can conclude that R_{ct} value is directly proportional to the concentration of G.M.E and this indicates that a passive film was formed on the Al alloy surface by the adsorption, which lead to a rise in %IE in HCl solution. While the data of C_{dl} is inversely proportional to G.M.E concentrations compared to that of blankthe solution, due to exchange water molecules by G.M.E which lead to an improve in the thickness of the formed electric double layer on the Al surface and/or lower in local dielectric constant [40, 41].

Table 4. Parameters obtained from EIS tests for Al alloy in 1.0 M HCl with and without different concentrations of G.M.E. at 25ºC

Inhibitor	[Inh] ppm	R_{ct} Ω Cm^2	C_{dl} x 10^6 Ω Cm^{-2}	Θ	%IE
Blank	0	1.7	21.0	---	---
Glycine Max extract	50	1.9	3.07	0.105	10.5
	100	2.4	2.91	0.292	29.2
	150	3.3	2.90	0.485	48.5
	200	6.5	2.74	0.738	73.8
	250	7.4	2.04	0.770	77.0
	300	9.7	1.80	0.824	82.4

3.4. Electrochemical Frequency Modulation (EFM) Measurements

EFM is considered as a nondestructive test for corrosion calculation which can measure the corrosion current value straight away with a small polarizing signal only and without previous information of Tafel slopes, which makes it a helpful method for online corrosion control [42]. The causality factors are considered as the main advantage of EFM because they act as an internal check for the validity of EFM measurement. The frequency spectrum of the current responses used in the calculation of the causality factors CF-2&3. The EFM of Al alloy in 1M HCl solution and in presence of G.M.E at 25ºC is shown in figure 7. The investigational EFM data were treated for the activation model, supposing that the corrosion potential does not interchange due to the polarization of the working electrode [43]. The current of corrosion (i_{corr}), (β_c and β_a) which represent the Tafel slopes and (CF-2 and CF-3) which represents the causality factors were calculated by the larger peaks. Gamry EFM 140 software was used to simultaneously determine these parameters and recorded in (table 5) showing that G.M.E protects the Al alloy corrosion in 1.0 M HCl with adsorption. Under various experimental conditions, the obtained CF is nearly equal to (2 and 3) which represent the theoretical values, meaning that the calculated data are in excellent quality [44]. IE_{EFM}%, which represents the inhibitor efficiency is directly proportional to G.M.E concentrations and was calculated as follows:

$$IE\%_{EFM} = \left[1 - \frac{i_{corr}}{i^o{}_{corr}}\right] x\ 100 \qquad (7)$$

Where the corrosion current densities are expressed by $i^o{}_{corr}$ and i_{corr} in without and with G.M.E, in that order.

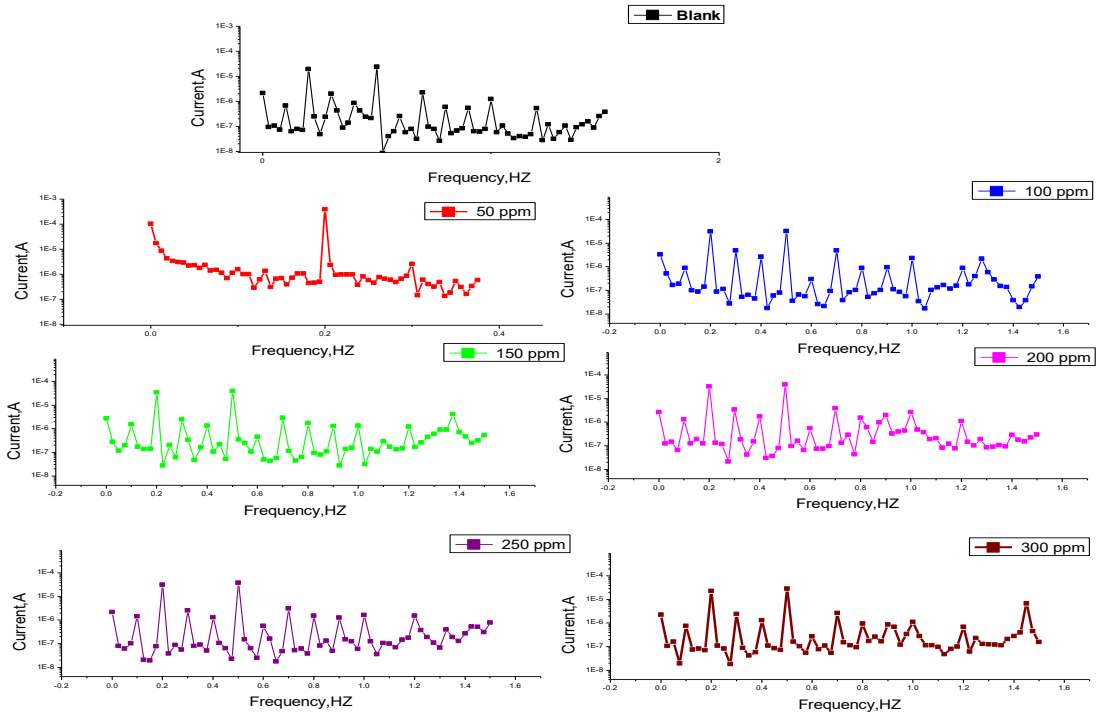

Figure 7. EFM spectrum for the corrosion of Al alloy in 1.0 M HCl with and without various concentrations of G.M.E. at 25°C

Table 5. Electrochemical data obtained from EFM for Al alloy in 1M HCl with and without various concentrations of G.M.E. at 25°C

Inhibitor	[Inh] ppm	i_{corr} m A Cm^{-2}	β_a mV dec^{-1}	β_c mV dec^{-1}	CF-2	CF-3	C.Rx10^3 mpy	Θ	IE%
Blank	0	1100	182	195	1.1	2.3	0.667	---	---
Glycine Max extract	50	566.5	48	63	2.051	2.8	17.79	0.485	48.5
	100	323.4	59	122	1.944	2.6	10.13	0.706	70.6
	150	317.9	76	179	2.086	2.5	9.977	0.711	71.1
	200	316.8	70	147	1.972	3.6	9.94	0.712	71.2
	250	311.3	63	125	1.957	2.6	9.768	0.717	71.7
	300	233.2	75	133	2.428	2.9	7.296	0.788	78.8

3.5. Adsorption Isotherms

The application of adsorption isotherms was used for studying the interface degree among an inhibitor and Al surface [43, 44]. Θ obtained from WL tests and were measured as a function of inhibitor concentration in order to give the adsorption isotherms. Then we plotted the values of Θ to fit the most suitable adsorption model [47]. Different isotherms contain Frumkin, Langmuir, and

Freundlich isotherms were made to fit experimental value. The greatest fitted by Langmuir isotherm as shown in figure 8 [48].

$$\frac{\theta}{1-\theta} = K_{ads}\, C \qquad (8)$$

Where (C) is the concentration in (g/L) of Glycine max in the bulk electrolyte, (θ=%IE/100).

The intercepts of Langmuir are associated with the adsorption free energy ΔG^{o}_{ads} then we could obtain the K_{ads} as the following equation:

$$K_{ads} = {}^{1}/_{55.5}\ \exp\left({}^{-\Delta G^{o}_{ads}}/_{RT}\right) \qquad (9)$$

Where 55.5 express the molar concentration of water in solution in M^{-1}.

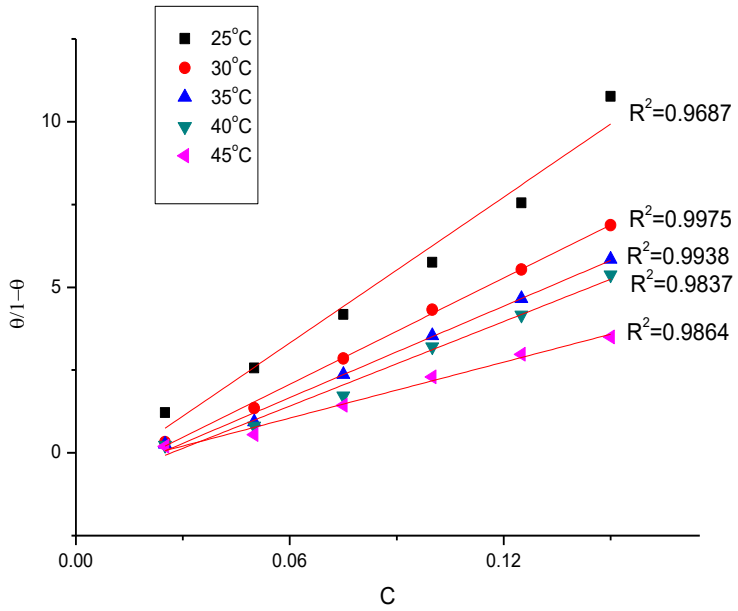

Figure 8. Langmuir plots for Al alloy in 1M HCl inclosing G.M.E and in presence of various concentrations at different temperatures

Plot of (ΔG^{o}_{ads}) Against T as in figure 9 gave the (ΔH^{o}_{ads}) and (ΔS^{o}_{ads}) according to equation 10:

$$\Delta G^{o}_{ads} = \Delta H^{o}_{ads} - T\,\Delta S^{o}_{ads} \qquad (10)$$

Table 5 obviously illustrates ΔG^{o}_{ads} excellent dependence on T, indicating the good correlation between the obtained thermodynamic data. The negative ΔG^{o}_{ads} sign data illustrate the spontaneity. Generally, ΔG^{o}_{ads} Values about -20 kJ/mol or lesser are corresponding to the electrostatic interaction among the charged molecules of G.M.E and the charged Al surface (physisorption), but those around -40 kJ/mol or greater are conforming to the charge sharing or transfer from plant extract molecules to the Al surface in order to form a coordinate kind of bond (chemisorption) [49]. The adsorption was established to be physical from the given data ofΔG^{o}_{ads}. Endothermic adsorption procedure ($\Delta H^{o}_{ads} > 0$) is based clearly on chemisorption [50], an exothermic procedure ($\Delta H^{o}_{ads} < 0$) may contain either chemisorption or physisorption or a mixture of both procedure. The calculated ΔH^{o}_{ads} values in the present for G.M.E adsorption in acidic solution indicating that, this inhibitor may adsorbed chemically

on Al surface. The $sign\ of\ \Delta S^{o}_{ads}$ in the presence of the inhibitor is positive which indicates that a lower in disorder occurred on going from reactants to the Al-adsorbed reaction complex [51].

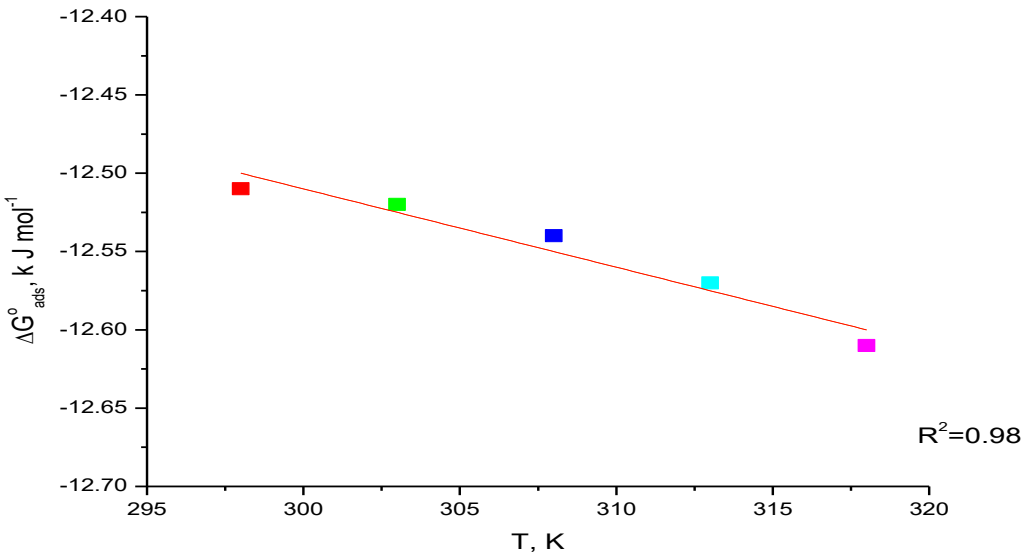

Figure 9. Variation of ΔG^{o}_{ads} vs T for G.M.E adsorption on Al alloy surface in 1.0M HCl at various temperatures

Table 6. Thermodynamic parameters of adsorption for Al alloy dissolution in 1.0M HCl at various temperatures

Temp. °C	**$K_{ads}x10^6$**	**$-\Delta G^{o}_{ads}$ k J mol^{-1}**	**$-\Delta H^{o}_{ads}$ k J mol^{-1}**	**ΔS^{o}_{ads} J mol^{-1} k^{-1}**
25	2.1	12.51	41.8	249.3
30	2.3	12.52		245.2
35	2.4	12.54		241.3
40	2.6	12.57		237.5
45	2.8	12.61		233.9

3.6 Kinetic-Thermodynamic Corrosion Parameters

At different temperatures (25-45°C), WL method was accomplished in the presence of various concentrations of G.M.E. It has been found that the corrosion rate is directly comparable to the temperature (table 1), which makes IE decreases with temperature. The corrosion parameter with and without G.M.E in the temperature range 25°C-45°C has been summarized in table 1. (E^{*}_{a}) Indicates the apparent activation energy for dissolution of Al alloy in 1.0 M HCl was measured by utilizing the Arrhenius equation from the slope of plots as follows:

$$\log K = \frac{-E^{*}_{a}}{2.303\,RT} + \log A \qquad (11)$$

Where the rate of corrosion is expressed by k and A is the Arrhenius pre-exponential factor.

E_a^* for the reaction of Al in 1M HCl rise with increasing G.M.E. Therefore, we can infer that the presence of the G.M.E. generates an energy barrier for the reaction of corrosion and this barrier rises with rising the extract concentration. Thus, the protection efficiency of the extract decreases noticeably with rising temperature. This result designates that the extract molecules adsorbed of on the Al alloy surface are physical in nature [52]. The entropy change (ΔS^*) and the enthalpy change (ΔH^*) both values can be calculated as follows:

$$K = \left(\frac{RT}{Nh}\right) exp\left(\frac{\Delta S^*}{R}\right) exp\left(\frac{\Delta H^*}{RT}\right) \qquad (12)$$

Where h expresses Planck's constant, k is the rate of corrosion, N is Avogadro number. A straight line should be given by plotting $\log {}^{K}/_{T}$ vs 1/T (figure 11), with a slope of $(\Delta H^*/2.303R)$ and an intercept of $\left[\log(R/Nh) + \frac{\Delta S^*}{2.303R}\right]$, from which ΔS^* and ΔH^* data can be measured (table 7). The ΔS^*positive sign data for the inhibitor indicated that during the rate determining step, activated complex signifies dissociation rather than an association step, which mean improve in disorder occurs during the course of transition from the reaction to the activated complex [53].

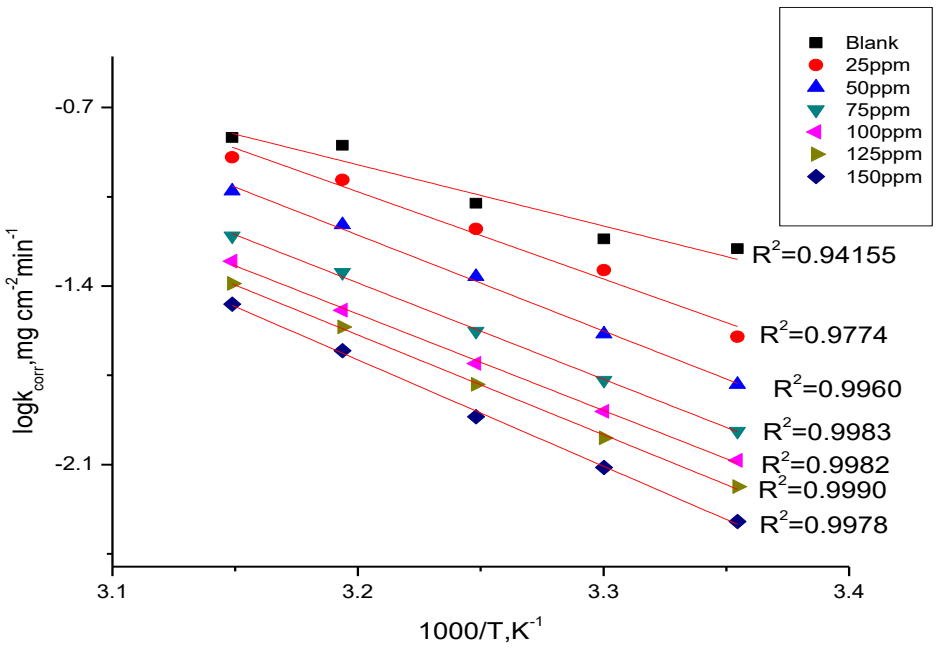

Figure 9. $\log K$ & 1/T plots for Al alloy in 1.0 M HCl with and without various concentrations of G.M.E. after 120 min.

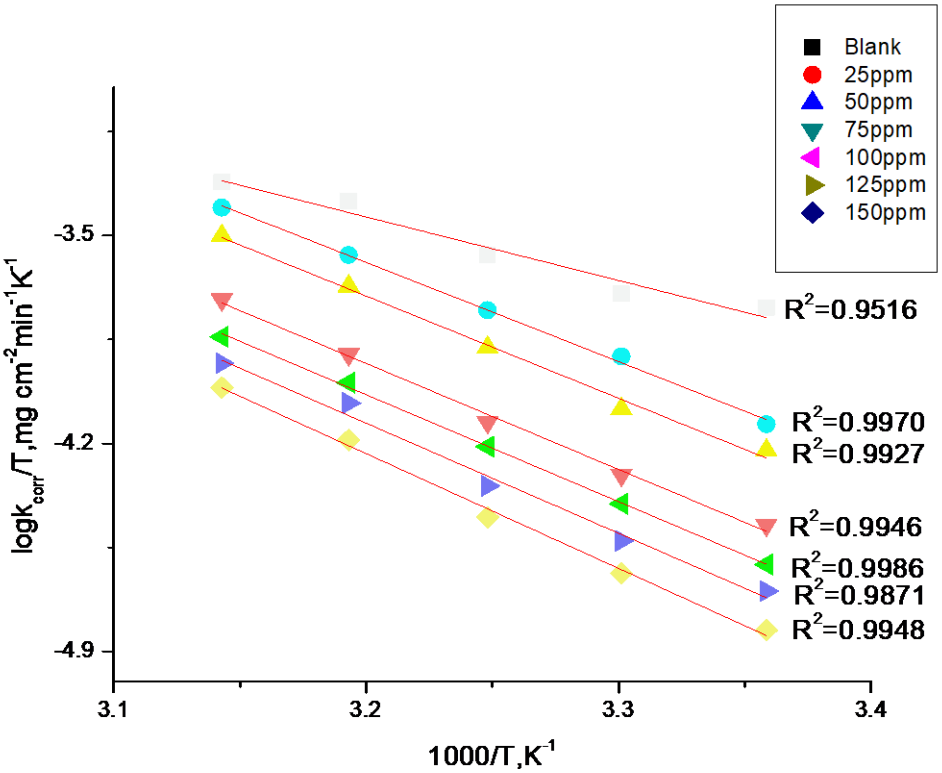

Figure 10.log K/T & 1/T curves for Al alloy in 1M HCl in the presence and absence of various concentrations of G.M.E. after 120 min

Table 7. Activation parameters for Al alloy dissolution in the presence and absence of various concentrations of G.M.E in 1.0M HCl after 120 min

Conc. Ppm	E_a^*, kJ mol^{-1}	ΔH^*, kJ mol^{-1}	ΔS^*, J mol^{-1}K^{-1}
0	132.7	127.4	144.2
50	155.7	162.6	257.6
100	161.8	159.3	254.6
150	162.0	159.5	249.8
200	162.2	159.6	246.3
250	164.4	161.9	243.3
300	166.0	164.4	245.1

3.7 Ssurface Analysis by SEM

Figure (11a) illustrates the surface portrait of the polish Al alloy before being exposed to an aggressive solution (blank). The coins were rare to microscopic analyses at x 2000. The micrograph

displays a characteristic addition. SEM image was shown in Figure (11b) for the surface of the Al alloy sample after dipping for 24 hours in an acidic environment. The image illustrates a strong damage to the specimen surface. The damaged areas are shown as black grooves in the sample with gray and white zones, which relate to the Al oxide. The highly oxidized phase perhaps formed in the air when dried up under no surface inhibition. Figure (11c) shows SEM images of the surface of another aluminum alloy coins after immersion in 1.0M HCl solution for the same time interval containing 300 ppm G.M.E. The image illustrates that, the protected alloy surface is smoother than the unprotected alloy surface, excellent protective film's exist on the Al surface. This indicates that G.M.E has the highest inhibition efficiency [54].

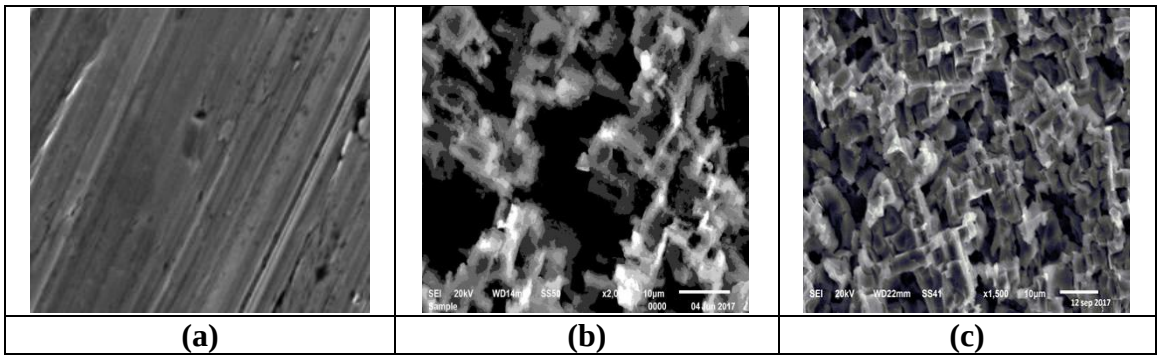

Figure 11. SEM Al alloy surface images (a) without dipping in HCl, (b)after 24 h of dipping in HCl and (C) after 24 h of dipping HCl + 300 ppm of G.M.E. at 25ºC

3.8 Corrosion Inhibition Mechanism

There are two kinds of interactions can illustrate the organic compound adsorption: chemisorption adsorption and physical. In general, both the electrically charged species in solution and charged Al surface are required in case of physical adsorption. The metal surface charge is in line for the electric field at the interface of the interface Al/solution. Otherwise, a chemisorption process includes charge transfer or charge sharing from the molecules of the inhibitor to the Al surface in order to form a coordinate kind of bond. This is imaginable in both negative and positive surface charge. Normally, two kinds of inhibitor mechanisms were proposed. One was the creation of polymeric complexes with Al ionsAl^{3+} reliant on the real system [55- 57]. The other was the adsorption of G.M.E on Al alloy surfaces [58, 59]. The protective action of G.M.E does happen by the simple blocking at the Aluminum alloy surface.

4. CONCLUSIONS

The next conclusions can be deduced from the overall experimental results:

1. The G.M.E as corrosion protection for Al alloy in 1.0M HCl shows a good performance.

2. The inhibiting action improves with the G.M.E concentration as shown from WL results and also decreases with the increase in temperature.

3. When G.M.E was added, a decreasing in double layer capacitance occurs. This confirms that the G.M.E molecules are adsorbed on Al alloy surface.

4. G.M.E inhibits the corrosion by being adsorbed on the Al alloy surface conferring to the equation of the Langmuir isotherm.

5. The obtained protection efficiencies by performing WL, EIS techniques and PP are all reasonably good matching.

References

1. G. Trabanelli, *Corrosion,* 47 (1991) 410.
2. P. Chatterjee, M. K. Banerjee, P. Mukherjee, *Ind. J Technol.,* 29(1991)191.
3. S. Rengamani, S. Muralidharan, M. A. Kulamdainathan, S. Venteatakrishna, *J.Appl. Electrochem.,* 24(1994)355
4. S. T. Arab, E. A. Noor, *Corrosion,* 49 (1993) 122.
5. G. K. Gomma, M. H. Wahdan, *Corros. Sci.,* 36(1994)79.
6. M. Ajmal, A. S. Mideen, M. A. Qurainhi, *Corros. Sci.,* 36(1994)97.
7. H. Z.M. Al-Sawaad, A. S.K. Al-Mubarak, A. M. Haddadi, *J. Mater. Environ. Sci.,* 1 (4) (2010) 227.
8. S. S. Abd El Rehim, H. Hassan, M. A. Amin, *Mater.Chem.Phys.,* 78 (2003) 337.
9. R. F. V. Villamil, P. Corio, J. C. Rubim, M. L. SilivaAgostinho, *J. Electroanal. Chem.,* 472 (1999) 112.
10. A. Khadraoui, A. Khelifa, L. Touafri, H. Hamitouche, R. Mehdaoui, *J. Mater. Environ. Sci.,* 4 (2013) 663.
11. M. Elachouri, M. S. Hajji, M. Salem, S. Kertit, R. Coudert, E. M. Essassi., *Corros.Sci.,* 37 (1995) 381.
12. H. Luo, Y. C. Guan, K. N. Han, *Corrosion,* 54 (1998) 619.
13. M. A. Migahed, E. M. S. Azzam, A. M. Al-Sabagh, *Mater. Chem.Phys.,* 85 (2004) 273.
14. M.M Osman, E. Khamis, and A. Michael, *Corros. Prev. Control,* 41(1994)60.
15. S. Bilgic, and N. Caliskan, *Appl. Electrochem.,* 31(2001)79.
16. A. S. Fouda, S. M. Rashwan, A. E. Mohammed and A. M. Ibrahim, *Egypt. J. Chem.,* 60(4) (2017) 491
17. T. Jain, R. Chowdhary, P. Arora, S. P. Mathur, *Bull Electrochem,* 21(2005)23
18. E. E. Ebenso, U. J. Ekpe, U. J Ibok, S. A. Umoren, E. Jackson, N. C. Oforka, O. K. Abiola, S. Martinez, *Trans SAEST,* 39(2004) 117.
19. G. D. Davis, J. Von Fraunhofer, *Mater Perform,* 42(2003) 56
20. A. Y. El-Etre, *CorrosSci,* 45(2003)2485
21. A.S.Fouda, Shady M. El–Dafrawy, Ali M. El-Azaly and Eslam S. El-hussieny (2018), J.Chem. Biol. Phys. Sci., 8(3) (2018) 325
22. A. S. Fouda, S. M. Rashwan, A. E. Mohammed and A. M. Ibrahim (2017) , Egypt. J. Chem., 60(4) (2017) 491
23. S. Ghahari, H. Alinezhad, G. A. Nematzadeh, M. Tajbakhsh, *Curr. Microbiol.,* 72 (4) (2017) 522.
24. A. S. Fouda, S. H. Etaiw, M. Hammouda, *J. Bio.Tribo. Corros.,* 3(2017)29
25. E. Mccafferty, *J.Electrochem. Soc.,* 150 (2003)342.
26. M. O. A. El Sheikh, G. M. El Hassan, A. H. El Tayeb, A. A. Abdallah, M. D. Antoun, *Planta Medica.,* 45 (1982) 116.
27. M. Eeva, J. P. Salo, K. M. Oksman-Caldentey,*J. Pharm. Biomed. Anal.,* 16(5) (1998) 717.

28. G. N. Mu, T. P. Zhao, M. Liu, T. Gu, *Corrosion*, 52 (1996) 853.
29. R. G. Parr, R. A. Donnelly, M. Levy, W. E. Palke, *J. Chem. Phys.*, 68(1978) 3801.
30. R. W. Bosch, J. Hubrecht, W. F. Bogaerts, B. C. Syrett, *Corrosion*, 57(2001) 60.
31. D. Q. Zhang, Q. R. Cai, X. M. He, L. X. Gao, G. S. Kim, *Mater. Chem. Phys.*, 114 (2009) 612.
32. H. P. Lee, K. Nobe, *J. Electrochem. Soc.*, 133 (1986) 2035.
33. Z. H. Tao, S. T. Zhang, W. H. Li, B. R. Hou, *Corros. Sci.*, 51 (2009) 2588.
34. E. S. Ferreira, C. Giacomelli, F. C. Giacomelli, A. Spinelli,*Mater. Chem.Phys.*,83 (2004) 129.
35. T. Paskossy, *J. Electroanal. Chem.*, 364 (1994) 111.
36. F. B. Growcock, J. H. Jasinski, *J. Electrochem. Soc.*, 136 (1989) 2310.
37. S. S. Abd El-Rehim, K. F. Khaled, N. S. Abd El-Shafi, *Electrochim. Acta*, 51 (2006) 3269.
38. M. Metikos, R. Hukovic, Z. Bobic,*J. Appl. Elactrochem.*, 24 (1994) 772.
39. A. Caprani, I. Epelboin, P. Morel, H. Takenouti, *proceedings of the 4th European system. on Corros. Inhibitors*, (1975)571.
40. J. Bessone, C. Mayer, K. Tuttner, W. Lorenz, *J. Electrochim. Acta*, 28 (1983) 171.
41. I. Epelboin, M. Keddam, H. Takenouti, *J. Appl. Electrochem.*, 2 (1972) 71.
42. A. V. Benedeti, P. T. A. Sumodjo, K. Nobe, P. L. Cabot, W. G. Proud, *Electrochim. Acta*, 40 (1995) 2657.
43. H. Ma, S. Chen, L. Niu, S. Zhao, D. Li,*J. Appl. Electrochem.*,32 (2002) 65.
44. X. H. Li, S. D. Deng,H. Fu, *J. Appl. Electrochem.*, 40 (2010) 1641.
45. M. Lagrenee, B. Mernari, M. Bouanis, M. Traisnel, F. Bentiss, *Corros. Sci.*, 44 (2002) 573.
46. E. Kus,F. Mansfeld, *Corros. Sci.*, 48 (2006) 965.
47. G. A. Caigman, S. K. Metcalf, E. M. Holt, *J.Chem. Cryst.*, 30 (2000) 415.
48. S. S. Abdel–Rehim, K. F. Khaled, N. S. Abd–Elshafi, *Electrochim. Acta*, 51 (2006) 3269.
49. J. O. Bockris, D. A. J. Swinkels,*J. Electrochem. Soc.*, 111 (1964)736.
50. W. J. Lorenz, F. Mansfeld, *Corros. Sci.*, 21(1981)647.
51. A. Yurt, G. Bereket, A. Kivrak, A. BalabanandB. Erk, *J. Appl.Electrochem.*, 35 (2005) 1025.
52. F. Bentiss, M. TraisnelandM. Lagrenee, *Corrosion Sci.*, 42 (2000) 127.
53. M. M. Saleh, A. A. Atia, *J. Appl. Electrochem.*, 36 (2006) 899.
54. L. Narvez, E. Cano, D. M. Bastidas,*J. Appl. Electrochem.*, 35 (2005) 499.
55. X. H. Li, S. D. Deng, H. Fu, *Corros. Sci.*, 51 (2009) 1344.
56. I. K. Putilova, S. A. Balezin, Y. P. Barasanik, *Metallic Corrosion Inhibitors, Oxford: Pergamon Press*, (1960) 30.
57. V. R. Saliyan, A. V. Adhikari,*Bull. Mater. Sci.*, 31 (2007) 699.
58. Y. Li, P. Zhao, Q. Liang, B. Hou, *Appl. Surf. Sci.*, 252 (2005) 1245.
59. A. H. Mehaute, G. Grepy, *Solid State Ionics*, 9–10 (1989) 17.